

Macrophage Rac1-IL-1 β Signaling in the Context of
Atherosclerotic Calcification and COVID-19 Infection

By

Cadence Lee

Sc.M., Brown University, 2021

Thesis

Submitted in partial fulfillment of the requirements for the Degree of Master of Science
in the Graduate Program of Biotechnology at Brown University

PROVIDENCE, RHODE ISLAND

October 2021

AUTHORIZATION TO LEND AND REPRODUCE THE THESIS

As the sole author of this thesis, I authorize Brown University to lend it to other institutions for the purpose of scholarly research.

Date 08/26/2021

Cadence Lee

Cadence Lee, Author

I further authorize Brown University to reproduce this thesis by photocopying or other means, in total or in part, at the request of other institutions or individuals for the purpose of scholarly research.


Date 08/26/2021

Cadence Lee

Cadence Lee, Author

This thesis by Cadence Lee is accepted in its present form by the Graduate Program in Biotechnology as satisfying the thesis requirements for the degree of Master of Science

Date 08/25/2021

Signature: 

Dr. Alan R. Morrison, Advisor,
Assistant Professor of Medicine

Date _____

Signature: Elizabeth O. Harrington, PhD
Digitally signed by Elizabeth O. Harrington, PhD
Date: 2021.08.25 15:48:34 -04'00'

Dr. Elizabeth Harrington, Reader, Associate
Dean for Graduate and Postdoctoral Studies
in the Division of Biology and Medicine

Date 08.25.2021

Signature: 

Dr. Gaurav Choudhary, Reader, Professor of
Medicine and Chief of Staff

Approved by the Graduate Council

Date _____

Signature: _____

Dr. Andrew G. Campbell, Dean of the Graduate
School

Acknowledgements

I would like to thank my program director, Dr. Jacquelyn Schell, for encouraging me to pursue my graduate education and for awarding me the Biotechnology Graduate Program Sc.M. Fellowship scholarship to support my coursework. I would also like to acknowledge my professors in the Department of Molecular Pharmacology, Physiology, and Biotechnology, for teaching me the classroom fundamentals to carry innovative science into my future career.

Thank you to my parents, who have provided endless support in all areas of my journey. My growth through Brown as an undergraduate and graduate student would not have been possible without the advice, encouragement, and love from my family.

I am honored that Dr. Harrington and Dr. Choudhary are serving as my thesis readers and committee members, and I am thankful for the time and support they have provided in not only completing my graduate degree, but also in my overall research endeavors at the Providence VA Vascular Research Laboratory. I would like to acknowledge the entire Morrison Laboratory for the help over the years, with a special thanks to Dr. Mantsounga for patiently teaching me the techniques and protocols to succeed in the lab.

Most of all, thank you to my advisor and mentor, Dr. Alan R. Morrison, for truly shaping my trajectory as a scientist. Under his mentorship in the past 3 years, I have learned more than I could have hoped. I will always be grateful for the guidance, career support, and life lessons that Dr. Morrison has shared with me. He serves as a leader and role model for what I aspire to become as a compassionate physician-scientist.

Table of Contents

Title Page	1
Authorization	2
Signature Page	3
Acknowledgements.....	4
Table of Contents	5
Table of Figures	6
Table of Tables.....	7
Abstract	8-9
Chapter 1: Introduction	10-15
Inflammatory atherosclerosis.....	10
Rac1 signaling in atherosclerotic calcification.....	13
IL-1 β and CAD in COVID-19 infection	15
Chapter 2: Materials and Methods.....	16-21
Animal models: myeloid IL-1 β and Rac1 KOs	16
Cloning hACE2 gene into mouse locus	21
Rac1 effectors leading to IL-1 β expression: NF- κ B and ROS	17
Near-infrared calcium imaging/histology	17
Lipid profile and ELISA quantification	18
Primary bone marrow derived macrophage culture	19
Cholesterol stimulation assay	19
Transfection	20
ChIP	20
PLA.....	21
Chapter 3: Results	22-32
Rac1 KO leads to decreased IL-1 β	22
Rac1 KO leads to decreased atherosclerotic calcification	23
Association of Rac1 and NF- κ B	26
IL-1 β and ACE2 expression	29
hACE2 mouse for studying CAD-related outcomes in COVID-19.....	31
Chapter 4: Discussion and Conclusion.....	33-36
References.....	37-45

Table of Figures

Figure 1: Macrophage Rac1 KO leads to reduced IL-1 β production.....22

Figure 2: Histological aortic sections of WT vs Rac1 KO.....24

Figure 3: Ex vivo calcium imaging of WT vs Rac1 KO aortas after HFD.....25

Figure 4: ROS and NF- κ B assays indicate Rac1 to act through NF- κ B.....26

Figure 5: ChIP data shows association between NF- κ B and IL-1 β promoter.....27

Figure 6: IL-1 β production with respect to nuclear localization of Rac1.....28

Figure 7: Macrophage IL-1 β KO demonstrates reduced ACE2 mRNA.....29

Figure 8: Plasmid map of a pUC19 vector containing the hACE2.....31

Table of Tables

Figure 6B: Table of ACE2 F0 founder mice.....31

Abstract: Macrophage Rac1-IL-1 β Signaling in the Context of Atherosclerotic Calcification and COVID-19 Infection, by Cadence Lee, ScM, Brown University, October, 2021

Objective: Previous models of progressive atherosclerotic calcification developed by the Morrison laboratory revealed that those models depend on macrophage Rac1 activity stimulating increased IL-1 β expression. We sought to define the mechanisms governing Rac1-induced IL-1 β expression and whether this pathway is involved in the natural progression of atherosclerosis in an experimental model of hyperlipidemia (*ApoE*^{-/-}). Moreover, we seek to define the impact of this inflammatory signaling pathway in the context of coronary artery disease (CAD) and COVID-19 infection.

Methods: We used novel mouse strains with tamoxifen-inducible, myeloid-specific knockouts of *Rac1* and *IL-1 β* . Animals were bred on an apolipoprotein E deficient, (*ApoE*^{-/-}) atherogenic background and fed a cholesterol supplemented, high fat diet for 18-20 weeks. Aortas were analyzed *ex vivo* for calcification by near-infrared conjugated bisphosphonate or Alizarin red histology. Primary bone marrow-derived macrophages (BMDMs) were treated in culture with LPS+Cholesterol to mimic physiological inflammasome stimulation. Subsequent analysis involved cytokine ELISA, NF- κ B and ROS assays, chromatin immunoprecipitation, and plasmid transfection. Due to limitations inherent in current animal models of SARS-CoV-2 infection, we generated a “humanized” ACE2 (*hACE2*) mouse strain, inserting human ACE2 mRNA sequence into the native mouse *ACE2* locus under regulation of its native promoter using CRISPR-Cas9 technology.

Results: Results confirm atherosclerotic calcification to be dependent on Rac1 as an upstream effector of IL-1 β -mediated atherosclerotic calcification. We further demonstrate that Rac1 acts through transcription factor NF- κ B to mediate IL-1 β expression. We have successfully cloned the *hACE2* gene into appropriate constructs for CRISPR-Cas9 mediated gene editing and have established F0 founders and F1 progeny, demonstrating successful breeding and that the *hACE2* allele is passed on in the germ line.

Conclusions: Rac1 acts through NF- κ B to increase IL-1 β -dependent atherosclerotic calcification. A novel humanized ACE2 mouse strain is being developed and will help to define the mechanism of CAD-mediated worsening outcomes in COVID-19 infection.

Chapter 1: Introduction

Inflammatory Atherosclerosis

Coronary artery disease from atherosclerosis is the leading cause of morbidity and mortality in the world.¹ The prevalence in the U.S. for men and women between the ages of 60-79 is 24% and 15%, respectively, and increases to 36% of men and 24% of women for those over 80.² Atherosclerosis is a process whereby lipid-laden plaques accumulate in the intimal layer of arterial blood vessels, with hyperlipidemia being a major risk factor for atherogenesis.³ Plaques can be broadly defined as regions within arterial tissue that have abnormally accumulated material that can include but not be limited to lipids, fibrotic material, cellular debris, and calcium deposits.³ In early plaque development, extracellular lipid accumulation occurs in the intima beneath the endothelial monolayer.⁴ Native LDL migrates from the vessel lumen into the subendothelial space and can be oxidized by a combination of lipid peroxidation by reactive oxygen species (ROS) and fragmentation of apolipoprotein B-100 (ApoB100).⁵ The oxidized LDL (oxLDL) is then phagocytosed by macrophages that have been recruited to the site of inflammation, via the class A (SR-A) or class B (SR-B) macrophage scavenger receptors.^{6,7} The oversaturation of cholesterol exceeds the macrophage cell's metabolic capacity, resulting in the formation of lipid-rich "foam cells", which proliferate proinflammatory signaling and recruitment of additional myeloid cells. Foam cells are primarily macrophages that have become highly enriched in LDL, which is stored as cytoplasmic liquid droplets, generating a foamy appearance under the microscope.⁸ Foam cells experience dysregulation of lipid metabolism, which can result in the precipitation of cholesterol microcrystals. Consequently, cholesterol microcrystals can lead to lysosomal instability, activating the NLRP3 inflammasome complex to promote the activation and secretion of the

mature form of the major proinflammatory cytokine, interleukin-1 β (IL-1 β), into the extracellular plaque environment.⁹⁻¹¹ IL-1 β plays a critical role, recruiting other pro-inflammatory cell types as well as promoting enhanced production of other cytokines such as IL-6 and C-reactive protein (CRP).¹² Thus, the growing atheroma accumulates cholesterols and lipids, cells (endothelial, mesenchymal, and immune), and cellular debris from stressed/necrotic cells, which continue to aggravate the underlying inflammatory state of the vessel wall.

Accumulation of these vascular plaques can result in narrowing of the arterial lumen, leading to a wide range of cardiovascular complications like coronary artery disease, peripheral artery disease, and cerebrovascular disease.³ Arterial narrowing can disrupt myocardial oxygen supply, blood pressure, cardiovascular stress, can cause complete thrombotic obstruction or occlusion, and myocardial infarction related to plaque rupture or erosion. Clinically, elevated calcium associated with the vascular plaques, as measured by cardiac computed tomography, is predictive for total atherosclerotic burden and all-cause mortality.^{13,14} On an individual plaque level, calcification and calcific composition of atherosclerotic plaque may also be a biomarker of the disease state.¹⁵ The type and composition, micro or macrocalcification, can affect the vulnerability of the plaque against rupture. Microcalcification involves M1 macrophage-facilitated calcium deposition through vesicle-mediated mineralization from macrophage and vascular smooth muscle cell (VSMC) apoptosis, and VSMC-to-osteoblast differentiation, with nodules of $<50 \mu\text{m}$.^{16,17} Macrocalcification is associated with M2 macrophage-facilitated calcium deposition via VSMC maturation and osteoblast differentiation, defined by nodules $\geq 50 \mu\text{m}$.¹⁷ Microcalcification or “spotty” calcification of the plaque is theorized to increase mechanical stress on the fibrous cap and has been associated with greater incidence of rupture. However, on an individual plaque basis, and somewhat surprisingly, dense, macroscopic accumulations of

calcification within the plaque has been associated with lower incidence of rupture and adverse cardiovascular events.¹⁸ Further research in this area is required to resolve this seemingly paradoxical relationship demonstrating that larger macro-calcium deposits appear more stable whereas “spotty” micro-deposits of calcium appear more vulnerable to rupture. When the atherosclerotic plaque does rupture leading to thrombosis, it contributes to incidence of myocardial infarction and stroke, two of the major causes of mortality around the world.^{19–21}

IL-1 β has been proven to be an important regulator in inflammatory atherogenesis.²² Evaluation of serum from atherosclerotic patients revealed a positive correlation between IL-1 β protein and mRNA levels with severity of disease.^{23,24} Its 33kD precursor form, proIL-1 β , is cleaved by caspase-1 into the 17kD active IL-1 β , which produces responses in a number of cell types, including endothelial cells, smooth muscle cells, and monocyte/ macrophages. In endothelial cells, IL-1 β -induced inflammatory response results in increased accumulation of adhesion molecules (ICAM-1, VCAM-1, MCP-1) and chemokines in the blood vessel intima, with consequent recruitment of inflammatory cells to the growing atheroma.^{25,26} IL-1 β also increases monocyte and macrophage gene expression of additional cytokines, such as IL-6, and self-expression to promote an inflammatory cycle with subsequent proliferation and differentiation of VSMCs. Increased IL-6 stimulates hepatocyte production of acute phase reactants like CRP, thrombotic fibrinogen and plasminogen activator inhibitor, further proliferating atherogenesis. Therefore, the IL-1 β acts through IL-6 to affect downstream production of CRP, a major biomarker of inflammatory cardiovascular disease, in the liver.²⁷ In primary aortic smooth muscle cells from the *ApoE*-deficient murine model of hyperlipidemia, recombinant IL-1 β promotes transcription of osteogenic factors (RUNX2, MSX2, SRY-Box 9 or

SOX9, OSX), and increases calcium deposition in cell culture matrix in a dose-dependent manner, supporting a role for IL-1 β in vascular calcification as well.²⁸

Rac1 Signaling in Atherosclerotic Calcification

The Rac family of GTPases, including Rac1, have been shown to play a fundamental role in a wide variety of cellular processes, including cellular motility and migration, cell transformation, axonal guidance, lamellipodium, actin cytoskeletal organization, membrane extension during phagocytosis, the induction of DNA synthesis and gene expression, cytokinesis and superoxide production.^{29–35} GTPases are key molecular switches and highly regulated by a number of factors, including 1) guanine nucleotide exchange factors (GEFs), which activate GTPases by catalyzing the exchange of guanosine diphosphate (GDP) to GTP; 2) GTPase-activating proteins (GAPs), which lead to inactivation of GTPases by accelerating intrinsic GTPase activity; and 3) GDP-dissociation inhibitors (RhoGDI1), which limit the access of GTPases to GEFs.³⁵ Newer roles for Racs, particularly in physiological settings of inflammation and atherosclerotic vascular disease continue to emerge.

As indicated by the term “small GTPase”, the Rac1 protein is small, averaging about 21 kDa in size. Small GTPases may have one or more post translational lipid modifications, a prenyl group or an acyl chain, both of which serve to assist in subcellular localization of these proteins.³⁶ Protein isoprenylation is defined as a stable, covalent modification of a protein with an isoprenoid moiety, either a C15 farnesyl or a C20 geranylgeranyl, which is linked by thioester bond to the carboxyl terminal cysteine residue.³⁷ Protein isoprenylation targets a specific carboxyl terminal CAAX box, where protein farnesyltransferase recognizes CAAX, where the A's are aliphatic amino acids, and protein geranylgeranyl transferase recognizes CAAL, where

the terminal amino acid is usually a leucine.^{38,39} Racs possess this key carboxyl terminal cysteine residue for geranylgeranylation, supporting localization to the inner plasma membrane or nuclear envelope.^{40,41} Protein acylation, which includes palmitoylation, is usually a 16 carbon saturated fatty acid modification on any cysteine of the protein.³⁹ Palmitoylation is not a necessary post translational modification for subcellular localization but increases avidity for the membrane and influences transforming activity by assisting in regulating nuclear localization, in a switch like mechanism.⁴²⁻⁴⁴ Palmitoylation also appears to block RhoGDI binding and can occur at the same terminal CAAX isoprenylation site.^{41 43} Interestingly, Rac isoprenylation is required for palmitoylation to occur.⁴⁵

Rac1 is largely pooled in the cytosol of the cell and primarily bound to RhoGDI1 in its inactive (GDP-bound) state.⁴⁶ RhoGDI1 is a key accessory protein that regulates Racs, by keeping them soluble in the cytosol in the GDP-bound, inactive form, preventing the exchange of GDP to GTP. RhoGDI1 also appears to shuttle Racs to and from the plasma membrane, where they can interact with various Rac GEFs.^{47,48} However, in the GTP-bound, active state, Rac1 signaling can affect cell growth and inflammatory stimulation through a variety of mechanisms. Rac1 can modulate gene transcription through the activation of NF- κ B, JNK, and p38 mitogen-activated protein kinase (MAPK), all of which induce activator protein-1 (AP1) transcription factors.⁴⁹ These transcription factors can upregulate the expression of proteins that control cell cycle progression induce G1/S progression.⁵⁰⁻⁵³ Through NF- κ B, Rac1 also mediates proinflammatory cytokine stimulation, like TNF- α and IL-1 β .^{28,54}

IL-1 β and CAD in COVID-19 Infection

Inflammation is a critical aspect of the presentation of COVID-19.⁵⁵⁻⁵⁷ Understanding the proinflammatory mechanisms that increase risk for viral infection is needed if targeted immunotherapies are to be successful. The ongoing COVID-19 pandemic is due, in part, to efficient binding of the SARS-coronavirus 2 (SARS-CoV2) novel pathogen spike protein to the human ACE2 receptor on the surface of cells. Though there is similarity in infectivity mechanism to previously identified coronaviruses that caused the SARS and MERS epidemics, the COVID-19 outbreak has created unprecedented global complications. As of August 2021, there have been over 199 million reported cases across the world with over 4.2 million deaths attributed to infection.⁵⁸ Studies observed disproportionate fatality in patients with comorbidities including diabetes, cardiovascular diseases, respiratory diseases, and the elderly. Hospitalized COVID-19 patients demonstrated broadly elevated inflammatory cytokine IL-1 β , and downstream effectors VEGF-A and IL-6.⁵⁹ We recently observed that cardiovascular risk factors like aging and DM increased inflammatory IL-1 β in primary macrophages with corresponding increase in quantified ACE2 mRNA. Given this observation, we hypothesize a mechanism of IL-1 β -induced ACE2 expression leading to increased macrophage infectivity and systemic virulence in experimental CAD models. We designed a “humanized” ACE2 mouse to study the impact of macrophage IL-1 β expression as a critical virulence factor in an *ApoE*-deficient model of atherosclerosis. A mouse susceptible to COVID-19 infection will help define the mechanisms of increased virulence in certain patient populations, leading to novel treatment strategies for patients afflicted with this disease. I will outline development of a novel humanized mouse model for COVID-19 infection to study the role of macrophage IL-1 β in the incidence of SARS-CoV-2 infection and CAD-related worsening outcomes.

Chapter 2: Materials and Methods

Animals

All experiments with animals were approved by the Providence VA Medical Center Institutional Animal Care and Use (IACUC). *ApoE*^{-/-}, *Rac1*^{fl/fl}, and *CSF1R*^{mercremer} mice were commercially available and purchased from The Jackson Laboratory and have been previously described.⁶⁰⁻⁶² *IL-1β*^{fl/fl} mice were generated by our own lab by CRISPR/Cas9 technology in partnership with Brown University's Mouse Transgenic and Gene Targeting Facility. They were then crossed with *CSF1R*^{mercremer} mice to generate a novel myeloid-specific, tamoxifen-inducible model. Male and female mice between 8 and 10 weeks old, were put on a high-fat diet (HFD; 20% fat by weight with 1.25% cholesterol; ENVIGO TD.02028) ad libitum for ≤20 weeks. Mice with an *ApoE*^{-/-}, *CSF1R*^{mercremer}, and either *Rac1*^{fl/fl} or *IL-1β*^{fl/fl} genotype were intraperitoneally (IP) injected with 2mg of tamoxifen every day for 10 days to induce macrophage *Rac1* or *IL-1β* gene deletion before HFD.

Cloning of hACE2 into the mouse locus

hACE2 sequence was acquired from a donor construct and used to design fragments and primers that were ordered through IDT. Cloning was performed following manufacturer protocols with the In-Fusion HD Cloning Kit (Takara Bio cat.102518). Briefly, gene fragments and primers were designed with 15bp extensions homologous to adjacent fragment and vector ends. These primers were used to amplify gene fragments by PCR, followed by gel band purification using the Nucleospin Gel and PCR Clean-up kit (Takara Bio cat.740986.20). Fragments were ligated into a pUC19 vector using the In-Fusion kit and subsequently, the plasmid construct was transformed into the kit's Stellar Competent Cells. Clones of interest were

isolated using blue-white colony screening on an X-Gal IPTG agar plate. Plasmids were amplified and purified using the EndoFree Plasmid Maxi Kit (Qiagen cat.12362). Candidate plasmids were determined by PCR, followed by verification sequencing at the Keck DNA Sequencing Lab at Yale. Subsequent CRISPR/Cas9 prep and embryo microinjection was performed at the Mouse Transgenic and Gene Targeting Facility at Brown University.

NF- κ B and ROS Assays

We used the the Amaxa Mouse Macrophage Nucleofector Kit (Lonza) to transfect BMDMs with the NF- κ B Firefly Luciferase Plasmid (Promega) and pRL-TK (plasmid renilla luciferase HSV-thymidine kinase promoter) Renilla control plasmid (Promega). Twelve hours after transfection, we stimulated the cells with LPS at 10 ng/mL for 2 hours and then treated them with 1000 μ g/mL cholesterol crystals. Cells were allowed to incubate in this treatment for another 12 hours. The cell lysates were used to evaluate luciferase activity, which was measured by Dual-Glo Luciferase Assay System (Promega). For the ROS Assay, BMDMs were primed under the same LPS and cholesterol crystal conditions, but were incubated for ≤ 3 hours at 37°C. Levels were determined using the ROS-GloTM H₂O₂ Assay (Promega) per manufacturer protocols.

Near-infrared calcium imaging and histology

48 hours prior to euthanasia, animals were intraperitoneally injected with 2 nmol of IRDye 680RD BoneTag Optical Probe (LI-COR; cat.926-09374). Mice were euthanized and their tissue was fixed with 4% paraformaldehyde (buffered neutral). Aortas were microdissected and subsequently imaged *ex vivo* with the Odyssey Imaging System and aortic calcification was

quantified with Image Studio Lite (LI-COR) —acquisition settings: (1) 700nm intensity, 3 (2) resolution of 21 microns, and (3) focus offset, 0 mm. Image LUTS was set from 50 to 1500, with a kappa of 0.2. We outlined the entire aorta and standardized the signal intensity to the area of the tissue.

For paraffin embedded histology, harvested aortas were fixed and cleaned of surrounding adipose tissue. A 3mm section of the ascending aortic arch was isolated and prepared for embedding and staining at the Brown University Molecular Pathology Core. Briefly, aortas were incubated in 70%, 95%, and finally 100% ethanol for 90 minutes at each concentration. Tissue was incubated in xylene for 2 hours, then embedded in paraffin at 60°C for 2 hours. Aortas were processed into 10- μ m sections on glass microscope slides. Hematoxylin and eosin (H&E), Masson's Trichrome, and Alizarin red staining was performed according to protocols by the Brown University Molecular Pathology Core. Imaging of positive stained sections was performed by brightfield microscopy, with subsequent analysis by Image J.⁶³

ELISA quantification and lipid profile

Lipid profile analysis was carried out by the Yale Mouse Metabolic Phenotyping Center for serum total cholesterol (TC), LDL (low-density lipoprotein), and triglyceride (TG) levels, with the Roche COBAS Mira Plus automated chemistry analyzer. Serum and supernatant IL-1 β was measured using ELISA kits (Biolegend) according to manufacturer's protocols, at a 1:32 dilution for serum and a 1:10 dilution for cell culture supernatant.

BMDM primary cell culture

BMDMs were harvested by *in vitro* differentiation of primary macrophages derived from femur bone marrow with an existing protocol that results in >97% CD11b^{hi}F4/80^{hi} cells.^{64,65} Briefly, mice were euthanized according to existing protocols and mouse femurs and tibiae were dissected. We washed the bones in 70% ethanol followed by fully supplemented RPMI 1640 medium (10% fetal bovine serum, 10 mmol/L HEPES at pH 7.4, 2 mmol/L L-glutamine, 100 units/mL penicillin, 10 µg/mL streptomycin, and 50 µM 2-ME [2-mercaptoethanol]). Red blood cells were lysed by ammonium-chloride-potassium (ACK) lysis buffer (0.15 M NH₄Cl, 1 mmol/L KHCO₃, 0.1 mmol/L Na₂EDTA at pH 7.4). Cells were pelleted and counted. BMDMs were resuspended and plated at 3.5x10⁶ cells/10 cm petri dish in fully supplemented RPMI with 30% (v/v) L929 cell-conditioned medium. Cells were allowed to adhere and become confluent over 6 to 8 days. After culturing, macrophages were harvested using PBS with 1 mmol/L EDTA. Previous analysis using this protocol has proven through flow cytometric analysis that the recovered cells were >97% CD11b⁺F4/80⁺.

Cholesterol Crystal Inflammasome Assay

The protocol for cholesterol crystal formation has been previously established.⁹ 20mg of cholesterol (Sigma) was dissolved in 10mL isopropanol and diluted with 15mL ddH₂O. Precipitated cholesterol crystals were pelleted and dried for 1 hour at 70°C. Pellets were finely ground, vortexed, and resuspended in 0.1% fetal bovine serum in PBS to a final concentration of 50 mg/mL. BMDMs were primed with LPS at 10 ng/mL two hours prior to treatment by addition of 1000 µg/mL of cholesterol crystals for 24 hours. Culture supernatants were collected for

subsequent analysis of IL-1 β levels by ELISA, per manufacturer protocols (BioLegend; catalog No. 432604).

Transfection

Transfection of BMDMs was carried out according to the manufacturer's instructions (Lonza, Cat.VPA-1009; Mouse Macrophage Nucleofector Kit) using plasmids described previously.⁶⁶ Briefly, 1×10^6 BMDMs were transfected with 2.5 μ g of plasmid DNA corresponding to wild-type Rac1 (Rac1), Rac1 with a poly-Q tail substitution in the C-terminal polybasic region (Rac1 NLSQ), constitutively active Rac1 (CA Rac1), or constitutively active Rac1 with a poly-Q tail substitution in the C-terminal polybasic region (CA Rac1 NLSQ). 3×10^6 of transfected cells were plated per well, and incubated for 12 hours at 37°C in fully supplemented RPMI 1640 medium. Cells were then stimulated with LPS+IFN γ and allowed to incubate for an additional 12 hours before sample harvest and analysis by ELISA (Biolegend).

Chromatin Immunoprecipitation

NF- κ B ChIP assay was carried out according to the manufacturer's kit instructions (Millipore, cat.12-295). In brief, 1.5×10^6 BMDM lysates treated with LPS+IFN γ 5 hours prior were histone cross-linked to DNA using formaldehyde (37%). Fixed cells were scraped, washed, and pelleted with PBS containing proteases inhibitors. Pelleted cells were lysed in SDS buffer, sonicated, and spun down. The supernatant was re-suspended in ChIP buffer and pre-cleared with a salmon sperm DNA/agarose bead mixture, then incubated overnight at 4°C with an NF- κ B p65 antibody (1:100; Cell Signaling Technology cat.8242) or an isotype control (1:50, R&D Systems cat.AB-105-C). In the morning, samples were washed and underwent reversal of

histone-DNA crosslinking by 5M NaCl for 4 hours at 65°C. DNA was recovered by phenol/chloroform extraction and ethanol precipitation. Site-specific primers for the IL-1 β promoter region were designed and ordered from IDT to evaluate the physical interaction between NF- κ B, Rac1, and the IL-1 β promoter by quantitative RT-PCR. Results were expressed as relative delta Ct of NF- κ B and Rac1 to their respective isotype control antibodies.

Proximity Ligation Assay

To demonstrate a complex between Rac1 and NF- κ B in adherent BMDMs, a proximity ligation assay kit will be used as per manufacturer protocols.⁶⁷⁻⁶⁹ BMDMs will be plated on coverslips at a density of 300,000 cells per coverslip and incubated in primary antibodies to Rac1 and NF- κ B. Secondary antibody probes will allow for ligation and subsequent hybridization. Resulting fluorescence will be quantified ImageJ.⁶³

Chapter 3: Results

Myeloid-specific Rac1 KO leads to decreased IL-1 β production

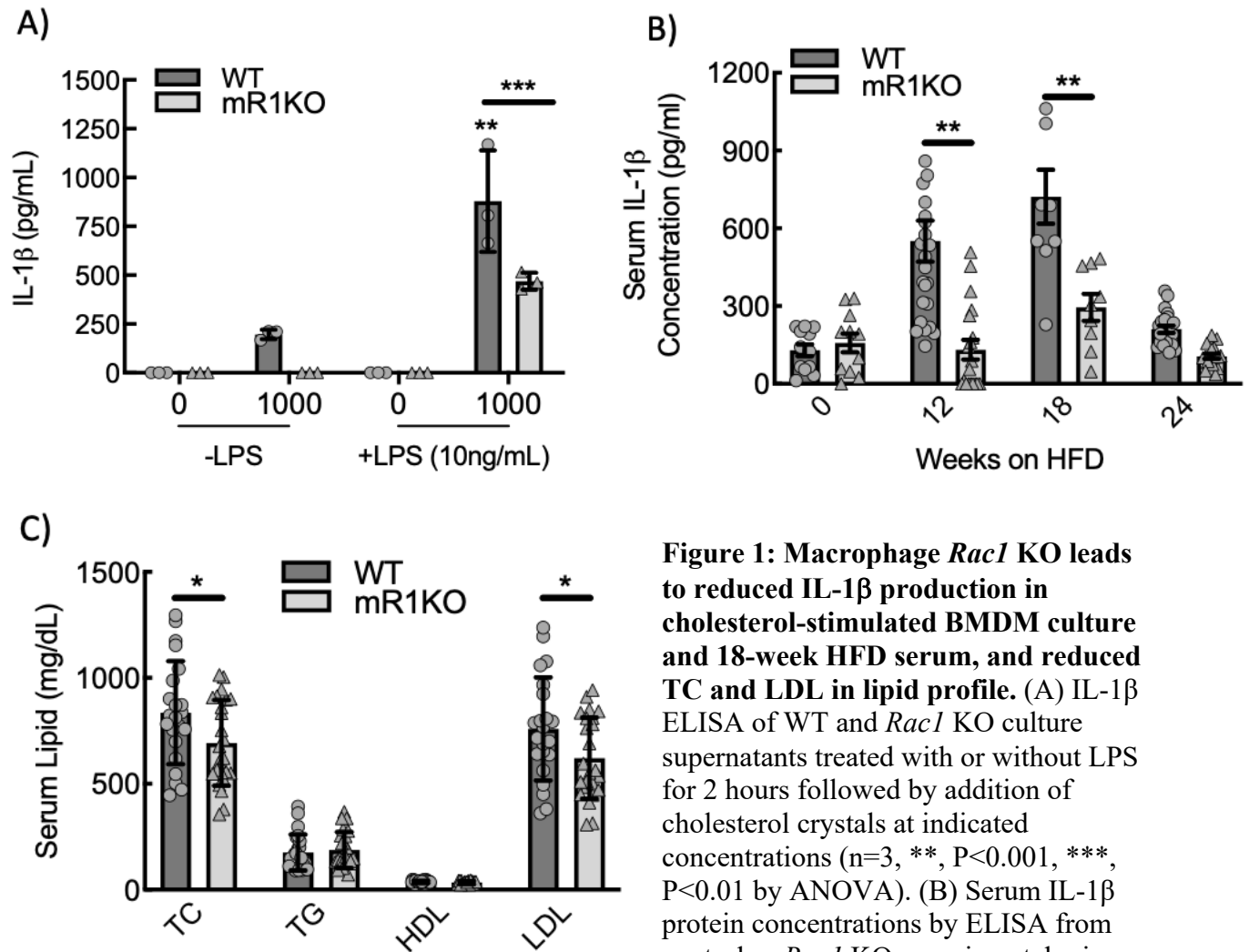


Figure 1: Macrophage *Rac1* KO leads to reduced IL-1 β production in cholesterol-stimulated BMDM culture and 18-week HFD serum, and reduced TC and LDL in lipid profile. (A) IL-1 β ELISA of WT and *Rac1* KO culture supernatants treated with or without LPS for 2 hours followed by addition of cholesterol crystals at indicated concentrations (n=3, **, P<0.001, *, P<0.01 by ANOVA). (B) Serum IL-1 β protein concentrations by ELISA from control or *Rac1* KO experimental mice on a high-fat diet (HFD) for indicated time**

points. (, Week 12 P<0.001 ANOVA; n=20; 10 males and 10 females, **, Week 18 P<0.001 ANOVA; n=20; 10 males and 10 females). (C) Analysis of lipid panel for mice 18-20 weeks on HFD, TC = Total Cholesterol, HDL = High-Density Lipoprotein, LDL = Low-Density Lipoprotein, TG = Triglycerides (TC and LDL P<0.05 by ANOVA; n=20 mice; 10 males and 10 females).**

We used a tamoxifen-inducible *CSF1R^{mercremer}*, myeloid-specific *Rac1* KO model to verify IL-1 β as a downstream effector of Rac1. Inflammasome stimulation with combined LPS and cholesterol crystal exposure showed that supernatant from *Rac1* KO BMDMs had a

significant reduction in IL-1 β cytokine production, determined by ELISA (Figure 1A). This trend is supported by IL-1 β ELISA serum analysis from mice over a high-fat diet (HFD) time course, where the *Rac1* KO animals demonstrated significantly reduced IL-1 β expression compared to the WT controls when challenged in an atherogenic context (Figure 1B). The difference in serum IL-1 β between groups was indistinguishable at 0 and 24 weeks, but became significant at 12 weeks and peaked at 18 weeks. The lipid panel analysis from the mouse serum indicates that triglyceride and LDL-C levels are also moderately reduced in the *Rac1* KO animals (Figure 1C). The assays altogether support the upstream effects of macrophage Rac1 on IL-1 β expression in an *ApoE*^{-/-} mouse model.

Macrophage Rac1 KO leads to decreased calcification

After 18 weeks on a HFD, aortas of *Rac1* KO and control mice were harvested for calcium analysis. Standard hematoxylin and eosin (H&E) staining was performed to evaluate plaque area, Masson's trichrome stain was used to evaluate collagen, and Alizarin red staining showed levels of calcium-containing osteocytes (Figure 2). As indicated by the quantification per plaque area in Figure 2A, the H&E and Masson's trichrome staining indicated no difference between the WT control and *Rac1* KO groups with respect to plaque area and collagen discrepancies (Figure 2A-B). However, the Alizarin red staining demonstrates a significant reduction in calcification in the *Rac1* KO group (Figure 2C), supporting the role of Rac1 in the calcification signaling pathway. The associated loss of Rac1 and atherosclerotic calcification is further supported by near-infrared calcium imaging of the entire aorta, where WT control animals showed significantly greater calcium deposition compared to both male and female *Rac1*

KO mice in *ex vivo* analysis (Figure 3). Quantification of both the near-infrared calcium imaging and Alizarin red staining support *Rac1* as an upstream effector of atherosclerotic calcification.

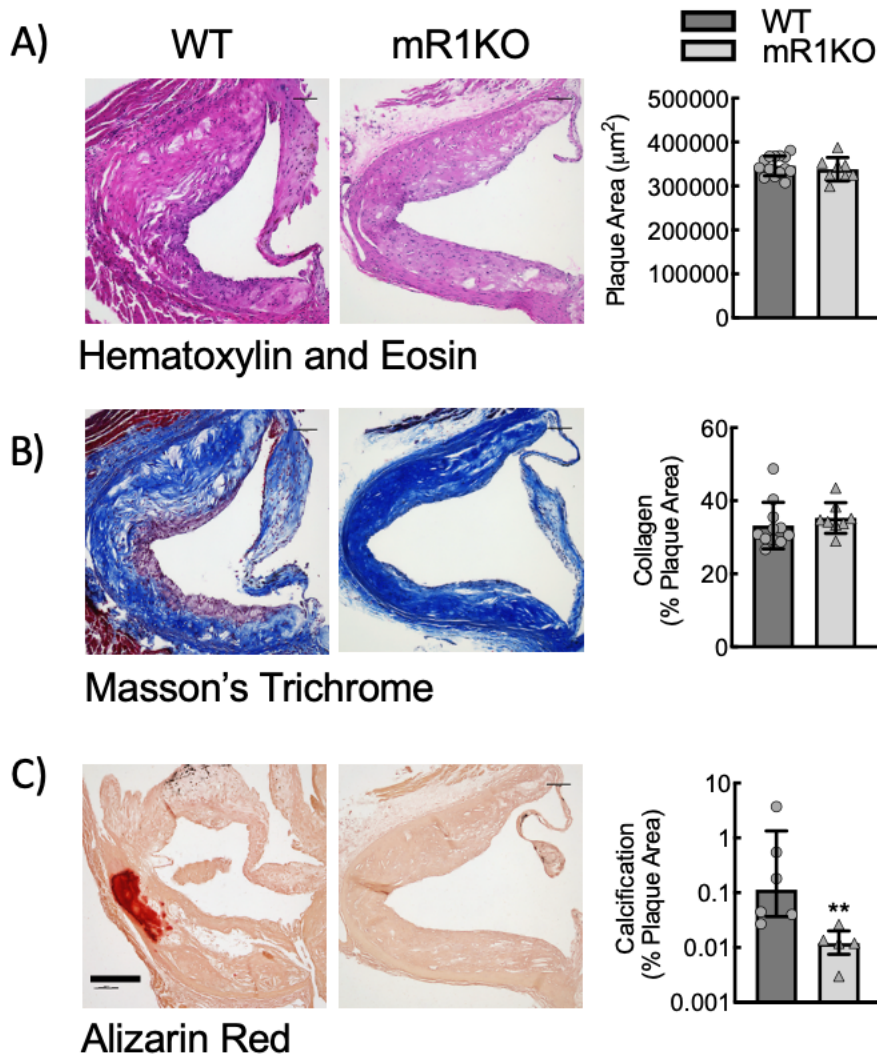


Figure 2: Macrophage *Rac1* KO leads to reduced calcification in the aorta, determined by staining. Histology of atherosclerotic plaques at the level of the aortic sinus of WT vs *Rac1* KO mice along with quantification of (A) plaque area defined by the border of smooth muscle cells in the vascular media and around the fibrous cap of the damaged endothelium evaluated by H&E staining, (not significant by ANOVA; n=22; 14 control, 8 experimental) (B) collagen percentage evaluated by Masson's Trichrome staining, (not significant by ANOVA; n=19; 11 control, 8 experimental) and (C) and calcification evaluated by Alizarin Red staining (**, P<0.05 by Mann-Whitney test; n=12; 6 control, 6 experimental), scale bar 100 μm .

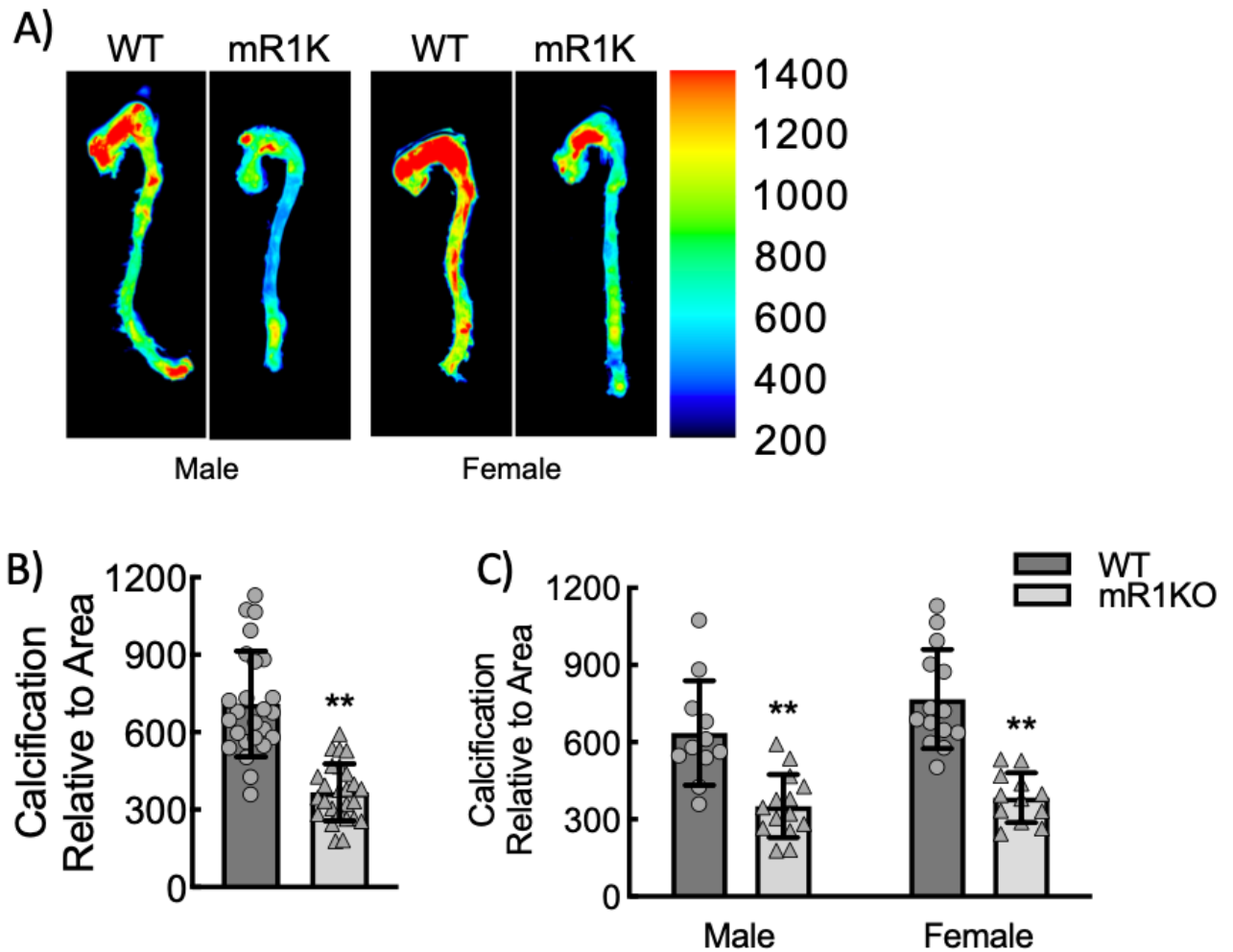


Figure 3: Macrophage *Rac1* KO leads to reduced calcification in the aorta, determined by *ex vivo* near-infrared calcium imaging. (A) Aortas of male and female *ApoE*^{-/-} *CSF1R*^{mcm} *Rac1*^{fl/fl}, *Rac1* KO or control mice harvested after high-fat diet (HFD) over 18-24 weeks with (B) quantification of calcification by near-infrared conjugated bisphosphonate signal relative to the area of the aorta (**, $P < 0.0001$ ANOVA; $n = 24$; 12 males and 12 females) and (C) by sex (Males; **, $P < 0.0001$ ANOVA; $n = 20$, 10 control, 10 experimental; Females; **, $P < 0.0001$ ANOVA; $n = 20$, 10 control, 10 experimental).

Rac1 acts through NF- κ B to increase IL-1 β expression

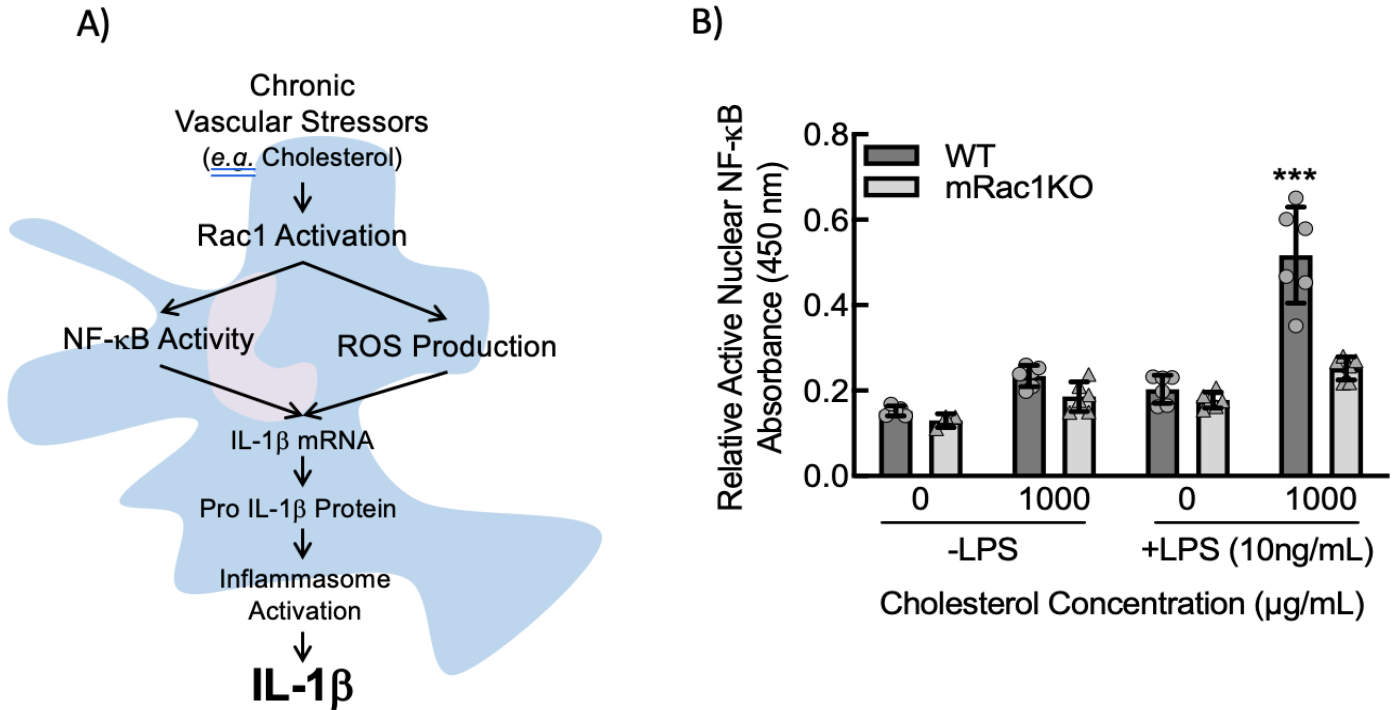


Figure 4: ROS and NF- κ B assays indicate Rac1 to act through NF- κ B, not ROS production. (A) Working model of chronic stressors such as cholesterol stimulation activating Rac1, leading to increased NF- κ B activity or ROS production, causing increased transcription of IL-1 β . (B) Relative nuclear NF- κ B activity measured by absorbance in primary BMDMs from control or *Rac1* KO experimental mice, primed with or without LPS (10 ng/ml) and exposed to cholesterol crystals (0 or 1000 μ g/mL) to induce inflammasome activation (**, P<0.001 ANOVA; n=6, 3 male, 3 female). (C) Relative signal as a measure of reactive oxygen species (ROS) production in primary mouse BMDMs from WT or *Rac1* KO experimental groups, stimulated with LPS+Cholesterol as described

previously. Negative control used a cell-free culture and positive control used menadione (50 μ M) treated cells (not significant by ANOVA; n=10 biological replicates from 8 mice; 4 males and 4 females).

Based on previous work, Rac1 is hypothesized to act through either NF- κ B activity or ROS production to exert its effects on IL-1 β .²⁸ Our working model proposes that vascular stressors such as cholesterol promote Rac1 activation, leading to either NF- κ B activation or ROS production, resulting in the downstream increase of IL-1 β we have previously determined (Figure 4A). We used the inflammasome assay (LPS and cholesterol crystal exposure) in BMDM cell culture systems to further investigate which pathway was significant in the Rac1-IL-1 β signaling axis. There was no difference in relative ROS production between the WT and *Rac1* KO cells (Figure 4C), whereas the *Rac1* KO group showed a significant reduction in relative active NF- κ B under LPS+cholesterol conditions (Figure 4B). This data indicates that NF- κ B activity is dependent on Rac1 whereas ROS production is not, suggesting that NF- κ B may be a key transcriptional activator of IL-1 β expression downstream of Rac1.

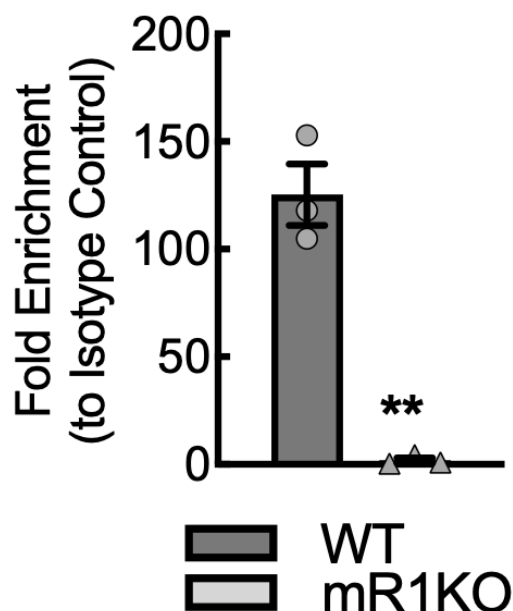


Figure 5: ChIP data shows association between NF- κ B and IL-1 β promoter. WT and *Rac1* KO BMDMs treated with LPS+IFN γ for 6 hours followed by NF- κ B ChIP and qRT-PCR for IL-1 β promoter region (**, P= 0.001, t-test, n= 3).

To confirm that NF- κ B acts as a transcriptional regulator for increased IL-1 β production, we used a chromatin immunoprecipitation assay followed by quantitative RT-PCR to determine Rac1-dependence of NF- κ B binding to the IL-1 β promoter. We performed ChIP using an antibody specific to NF- κ B as well as isotype control and then carried out quantitative RT-PCR for the IL-1 β promoter using primers specific to the DNA binding region for NF- κ B in lysates from both WT and *Rac1* KO BMDMs. Among 3 replicates, there was a significant difference between the fold enrichment compared to isotype control between the WT and *Rac1* KO cell lysates (Figure 5). The KO cells demonstrated equal Ct values for the IL-1 β promoter region between the NF- κ B and isotype control conditions, whereas the WT cell lysate demonstrated a significant difference in the detection of the IL-1 β promoter region between the NF- κ B and isotype control antibodies. This data supports our hypothesis that NF- κ B binds to the IL-1 β promoter in a Rac1-dependent manner, since the detection of the IL-1 β promoter region DNA by qRT-PCR was dependent on the presence of Rac1 in the WT control condition.

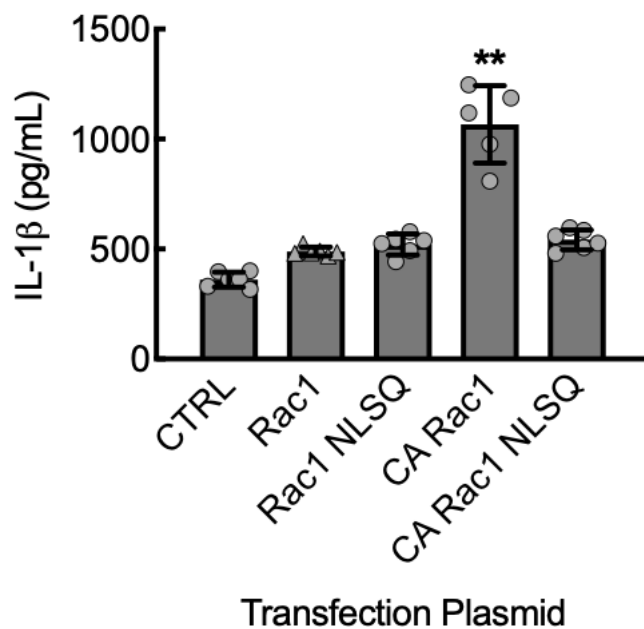


Figure 6: Transfection with Rac1 plasmids reveals a role of Rac1 nuclear localization in IL-1 β production. WT BMDMs were harvested and cultured for 6 days, then transfected with indicated plasmids: Rac1 with intact nuclear localization sequence, Rac1 NLSQ = Rac1 with a poly-Q substitution for the nuclear localization sequence, CA Rac1 = constitutively active Rac1, CA Rac1 NLSQ = constitutively active Rac1 with a poly-Q substitution for the nuclear localization sequence (n=6 replicates, **, P<0.0001 by ANOVA). 12 hours post-transfection, cells were treated with LPS+INF γ to stimulate the inflammasome, then supernatant was evaluated for IL-1 β by ELISA.

Transfection of wild-type BMDMs with constitutively active mutant of Rac1 (CA Rac1) reveals increased IL-1 β production and knockout of the nuclear localization sequence for CA Rac1 abrogates the effects of IL-1 β production, suggesting that Rac1 nuclear localization is required for the effects on IL-1 β expression (Figure 6). Ongoing studies are in progress, using a proximity ligation assay system, to determine if Rac1 forms a complex with NF- κ B, to chaperone it to the nucleus to perform its transcriptional function.

ACE2 receptor expression appears dependent on IL-1 β expression

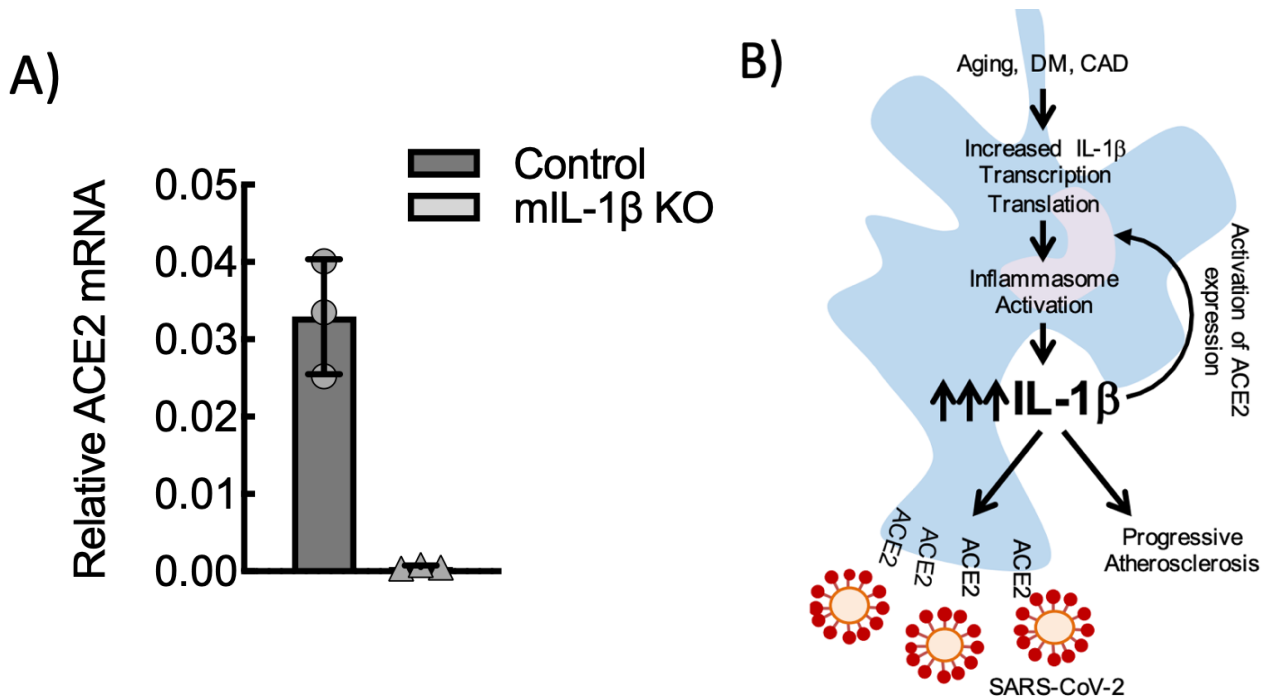
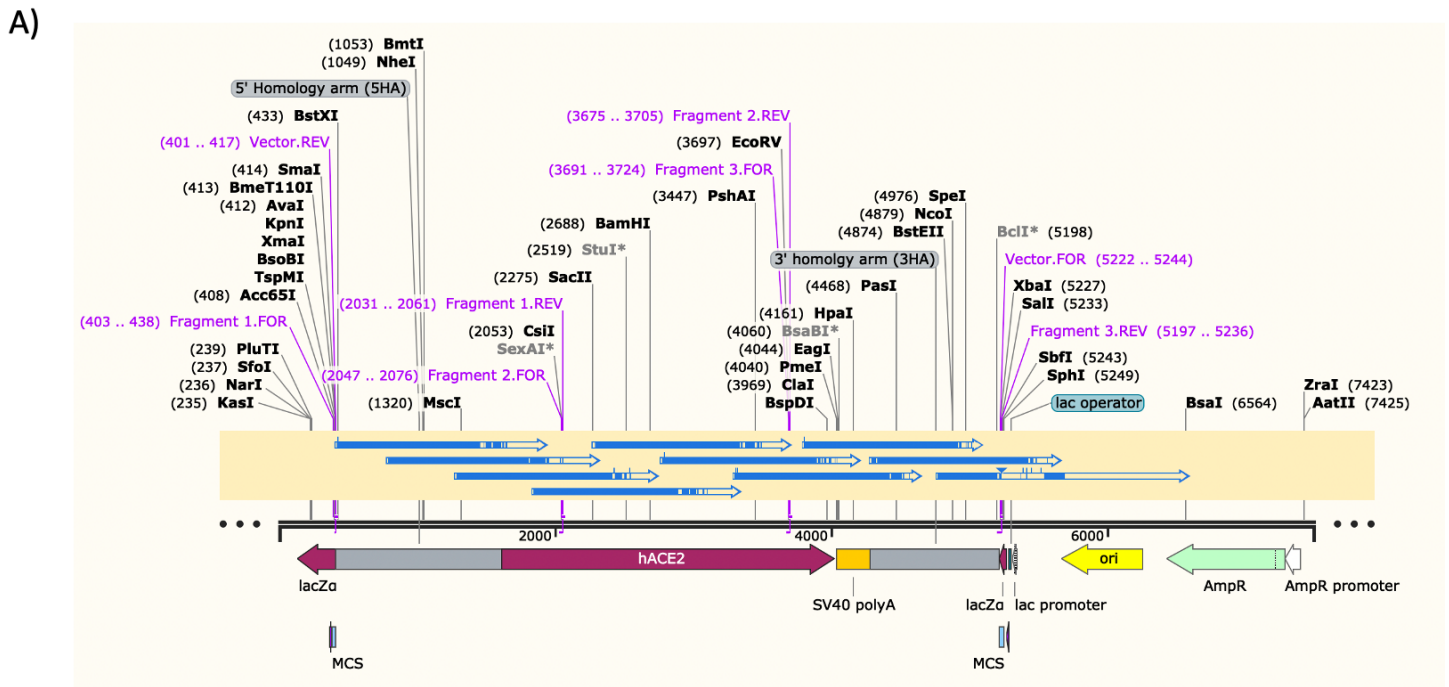


Figure 7: Macrophage IL-1 β KO demonstrates reduced ACE2 mRNA. (A) Real-time PCR quantification of GAPDH-normalized ACE2 mRNA expression in BMDMs from control or myeloid *IL-1 β* -deleted mice stimulated with LPS+IFN γ (**, P<0.002 t-test; n=3 mice, 2 males and 1 female). (B) Working model depicting comorbidities associated with increases in IL-1 β , causing increased expression of ACE2 and consequent increased cellular infection by SARS-CoV-2.

Understanding that Rac1-IL-1 β signaling axis is critical to atherosclerosis and atherosclerotic calcification may open the door to new targeted treatment strategies. Given that we seek to further elucidate the mechanism by which this Rac1-IL-1 β axis affects virulence of COVID-19 in the context of coronary disease, we assessed dynamic macrophage expression of the ACE2 receptor, which allows cellular entry of SARS-CoV-2. Preliminary qRT-PCR data from BMDMs stimulated with LPS+INF γ from vehicle control injected wild-type or tamoxifen-induced macrophage IL-1 β KO mice revealed that ACE2 mRNA expression is eliminated in the absence of macrophage IL-1 β (Figure 7A). This supports our working model that elevated IL-1 β , seen in inflammatory states such as atherosclerosis, may increase ACE2 receptor expression, thereby increasing cellular infection of COVID-19 infection and potentially worsening outcomes (Figure 7B).

Verification of a “humanized” ACE2 mouse model for studying IL-1 β and atherosclerosis in COVID-19

Figure 8: Donor template preparation and F0 founders of the “humanized” ACE2 mouse model. (A) Plasmid map and sequencing verification of a pUC19 vector containing the hACE2 gene for CRISPR-Cas9 microinjection. (B) Table of verified F0 founders containing the hACE2 insert. Mice #90 and #94 were generated using a single strand DNA donor, resulting in higher confidence that they do not contain undesired concatemers, multiple inserts linked in series.



B)

F0 mouse ID	DOB	Gender	Note
#31	4/16/21	Female	All good
#46	4/20/21	Male	Mosaic M249K (check F1 for a separation of correct sequence)
#90	6/30/21	Female	Generated with single strand DNA donor, no undesired concatemers
#94	6/30/21	Female	Generated with single strand DNA donor, no undesired concatemers

To study the association of Rac1, IL-1 β , and atherosclerosis in COVID-19 infection, we created a novel “humanized” mouse that expresses ACE2 under its native promoter in order to be adequately infected by SARS-CoV-2. 10 sequencing primers were used to verify the correct sequence (indicated by blue arrows) of the *hACE2* gene into the pUC19 vector (Figure 8A). Flanking mouse homology-arm segments (indicated in grey) are also necessary for the proper localization of the gene insert. The human ACE2 insert itself (indicated in maroon) is oriented between the flanking ends, followed by an SV40 Polyadenylation tail (indicated in orange) that serves as the termination sequence and stabilizes the mRNA to enhance translation *in vivo*. Following design, cloning, and verification, this plasmid was used to create the novel mouse model utilizing CRISPR-Cas9 genome editing. Within 3 months, resulting F0 founders were identified (Figure 8B). The founders were crossed with C57BL/6J mice to produce the F1 progeny, which are currently being backcrossed to each other to create homozygous *hACE2* mice. Airway epithelial cells from wild-type (mouse *ACE2*), heterozygous *hACE2*, and homozygous *hACE2* mice will be assessed for the presence of the mouse vs. human ACE2 RNA and protein expression, by immunohistochemistry and immunoblotting, using species-specific targeted anti-ACE2 antibodies.

Chapter 4: Discussion and Conclusions

Atherosclerosis is a chronic inflammatory immune-mediated disease, and treatment of atherogenesis should reflect our current knowledge of immune-related pathogenesis. In summary, I have observed that endogenous macrophage Rac1 acts through NF- κ B to increase IL-1 β expression, leading to subsequent atherosclerotic calcification. The results from *Rac1* KO BMDM cultures and serum analyses support macrophage Rac1 as an upstream effector of IL-1 β expression. Histology and *ex vivo* calcium imaging provide further support for the hypothesis that the Rac1-IL-1 β axis mediates atherosclerotic calcification. Transfection with CA Rac1 identified Rac1 nuclear localization as critical for increasing IL-1 β expression. Nuclear NF- κ B activity ELISA assays and quantitative RT-PCR data post-ChIP demonstrated that macrophage Rac1 acts through NF- κ B to promote IL-1 β transcription, and further experiments are required to determine whether Rac1 may be acting as a chaperone in a complex with NF- κ B to help localize NF- κ B to the nucleus and subsequently to the IL-1 β promoter. Proximity ligation assays are in progress to determine whether Rac1 and NF- κ B can form a complex under conditions that stimulate IL-1 β production.

This observation of a Rac1-IL-1 β -mediated increase in atherosclerotic calcification is supported by prior *in vitro* studies on the relationship between inflammatory macrophages and downstream cytokine activation of vascular smooth muscle cells to an osteoblast, calcific phenotype, though our data is the first study in the context of an *in vivo* model of experimental atherosclerosis.^{28,70-72} Our data and use of a conditional, myeloid-specific Rac1 KO add to the literature by providing a mechanistic understanding of the Rac1-NF- κ B interaction. While our work supports Rac1's ability to modulate gene transcription through NF- κ B, which has been documented in the past⁴⁶, our studies add the additional dimension of demonstrating Rac1 is

required for active NF- κ B to localize to the nucleus and specifically to the IL-1 β promoter. Previous work, using transient expression with a constitutively active plasmid of Rac1, the G12V mutant, demonstrated increased NF- κ B transcriptional activity by a nonspecific, NF- κ B reporter system of promoter-driven luciferase expression in the context of bacteria-derived, HKSA-stimulation of 293-TLR2 cells, and thus was unable to study the nuclear localization or specific promoter localization of NF- κ B.^{73,74} Our transfection data supports the findings of these prior studies, that activation of Rac1 determines NF- κ B activity, but adds the additional evidence in primary cell assays that the Rac1 nuclear localization sequence is required for nuclear-localized NF- κ B activity and that Rac1 determines binding specifically to a chromosomal seed site, namely the IL-1 β promoter. Thus, these experiments contribute additional knowledge suggesting a chaperone function concerning the mechanistic relationship between Rac1 and NF- κ B and moreover indicating for the first time that Rac1 may play a role as a transcriptional co-factor for NF- κ B in promotion of IL-1 β transcription. In the context of atherosclerotic calcification, as previously mentioned, the type of calcium deposit, whether micro- or macrocalcification, has an impact on stability of disease.¹⁸ Thus, clarifying this novel mechanism of Rac1-dependent, IL-1 β -mediated calcification is critical to the development of new types of treatment strategies, targeting the composition and stability of atherosclerotic plaques in patients with CAD.

In light of the recent global pandemic, it is also important to understand these mechanisms in the context of COVID-19 infection. Research on the inflammatory pathways that influence disease states such as CAD may help inform treatment strategies for patients with inflammatory comorbidities who suffer worsened outcomes. For translational research, development of an efficient and effective animal model is essential for evaluating the molecular basis of the disease. There are a variety of existing mouse models that attempt to circumvent the

human and mouse ACE2 binding discrepancies in COVID-19 susceptibility. Of the models commercially available in the U.S., the transgenic *K18-hACE2* model, the *hACE2-KI* model, and the ACE2-GR model are the frontrunners.^{75,76} While the *K18-hACE2* mice exhibit successful infection with the virus, the expression of human ACE2 is driven by the human keratin 18 (*KRT18*) promoter, making expression of the human protein specific to epithelial cells such as those in the airway, liver, kidney, and GI. Some concerns about this the model include the lack of K18 expression in endothelial cells and immune cells, limiting its application as a model for studying systemic vasculopathy or immune cell infection observed in patients in the context of COVID-19.⁷⁶ On the other hand, the recent development of *hACE2-KI* and ACE2-GR models allow for expression of human ACE2 under the regulation of the endogenous mouse promoter, using a neomycin resistance (neo) cassette insertion at the junction of the human *ACE2* and the mouse *Bmx* genes for development.^{77,78}

My work to create and verify a novel human ACE2 mouse model utilizing CRISPR-Cas9 to insert the human *ACE2* gene into the mouse locus will provide support for the preclinical and translational research in studying COVID-19. An advantage of this novel mouse model over the *K18-hACE2* model includes its expression of the human ACE2 under the regulation of the endogenous mouse promoter, also allowing the expression of the protein in cells of tissues other than strictly epithelial and therefore more closely mimicking the human phenotype. Since this model uses CRISPR-Cas9 in site-directed mutagenesis, the resulting mice may have a different phenotypic response to SARS-CoV-2 infection when compared to the *hACE2-KI* and ACE2-GR mice that utilized a neo cassette development approach. Using the original F0 founders bred against C57BL/6 WT mice, I have begun the process of backcrossing the F1 progeny to develop experimental cohorts. We plan to evaluate RNA and protein levels to verify expression of the

human ACE2 receptor, which will be followed by verification of the mice susceptibility to COVID-19 infection at the Tufts New England Regional Biosafety Laboratory BSL-3 facility. Following verification, I anticipate that this mouse model will aid in the study of inflammatory and cardiovascular comorbidities on virulence during COVID-19 and help to build on therapeutic insights gained from the observations of our Rac1-IL-1 β signaling axis in atherosclerotic calcification.

References

1. Mozaffarian D, Benjamin EJ GA. Heart disease and stroke statistics--2015 update: a report from the American Heart Association. *Circulation*. 2015;131(4):e29-e39. doi:10.1161/CIR.000000000000152
2. Yazdanyar A NA. The burden of cardiovascular disease in the elderly: morbidity, mortality, and costs. *Clin Geriatr Med*. 2009;25(4):563-577.
3. Libby P, Buring JE, Badimon L, et al. Atherosclerosis. *Nat Rev Dis Prim*. 2019;5(1):1-18. doi:10.1038/s41572-019-0106-z
4. Kramsch DM, Franzblau C HW. The protein and lipid composition of arterial elastin and its relationship to lipid accumulation in the atherosclerotic plaque. *J Clin Invest*. 1971;50(8):1666-1677.
5. Madamanchi, Nageswara R. et al. Oxidative Stress and Vascular Disease. *Arterioscler Thromb Vasc Biol*. 2005;25(1):29-38.
6. Kzhyshkowska J, Neyen C, Gordon S. Role of macrophage scavenger receptors in atherosclerosis. *Immunobiology*. 2012;217(5):492-502. doi:10.1016/j.imbio.2012.02.015
7. Podrez EA, Febbraio M, Sheibani N, et al. Macrophage scavenger receptor CD36 is the major receptor for LDL modified by monocyte-generated reactive nitrogen species. *J Clin Invest*. 2000;105(8):1095-1108. doi:10.1172/JCI8574
8. Li AC, Glass CK. The macrophage foam cell as a target for therapeutic intervention. *Nat Med*. 2002;8(11):1235-1242. doi:10.1038/nm1102-1235
9. Duewell P, Kono H, Rayner KJ, et al. NLRP3 inflammasomes are required for atherogenesis and activated by cholesterol crystals. *Nature*. 2010;464(7293):1357-1361. doi:10.1038/nature08938

10. Geng YJ, Phillips JE, Mason RP, Casscells SW. Cholesterol crystallization and macrophage apoptosis: Implication for atherosclerotic plaque instability and rupture. *Biochem Pharmacol.* 2003;66(8):1485-1492. doi:10.1016/S0006-2952(03)00502-1
11. Rajamäki K, Lappalainen J, Öörni K, et al. Cholesterol crystals activate the NLRP3 inflammasome in human macrophages: A novel link between cholesterol metabolism and inflammation. *PLoS One.* 2010;5(7):1-9. doi:10.1371/journal.pone.0011765
12. Lopez-Castejon, Gloria and DB. Understanding the mechanism of IL-1 β secretion. *Cytokine Growth Factor Rev.* 2011;22(4):189-195.
13. Budoff MJ, Mao S, Zalace CP, Bakhsheshi H OR. Comparison of spiral and electron beam tomography in the evaluation of coronary calcification in asymptomatic persons. *Int J Cardiol.* 2001;77(2-3):181-188.
14. Rennenberg RJ, Kessels AG, Schurgers LJ, van Engelshoven JM, de Leeuw PW K, AA. Vascular calcifications as a marker of increased cardiovascular risk: a meta-analysis. Vascular health and risk managem. *Vasc Health Risk Manag.* 2009;5(1):185-197.
15. Dweck MR, Aikawa E, Newby DE, et al. Noninvasive Molecular Imaging of Disease Activity in Atherosclerosis. *Circ Res.* 2016;119(2):330-340.
doi:10.1161/CIRCRESAHA.116.307971
16. Shioi A, Ikari Y. Plaque calcification during atherosclerosis progression and regression. *J Atheroscler Thromb.* 2018;25(4):294-303. doi:10.5551/jat.RV17020
17. Irkle A, Vesey AT, Lewis DY, et al. Identifying active vascular microcalcification by 18F-sodium fluoride positron emission tomography. *Nat Commun.* 2015;6(May).
doi:10.1038/ncomms8495
18. Criqui MH, Denenberg JO, Ix JH, et al. Calcium density of coronary artery plaque and

- risk of incident cardiovascular events. *JAMA - J Am Med Assoc.* 2014;311(3):271-278.
doi:10.1001/jama.2013.282535
19. Bentzon JF, Otsuka F, Virmani R, Falk E. Mechanisms of plaque formation and rupture. *Circ Res.* 2014;114(12):1852-1866. doi:10.1161/CIRCRESAHA.114.302721
 20. Donkor ES. Stroke in the 21st Century: A Snapshot of the Burden, Epidemiology, and Quality of Life. *Stroke Res Treat.* 2018;2018. doi:10.1155/2018/3238165
 21. Ioacara S, Popescu AC, Tenenbaum J, et al. Acute myocardial infarction mortality rates and trends in Romania between 1994 and 2017. *Int J Environ Res Public Health.* 2020;17(1):1-9. doi:10.3390/ijerph17010285
 22. Grebe A, Hoss F, Latz E. NLRP3 inflammasome and the IL-1 pathway in atherosclerosis. *Circ Res.* 2018;122(12):1722-1740. doi:10.1161/CIRCRESAHA.118.311362
 23. Galea J, Armstrong J, Gadsdon P, Holden H, Francis SE HC. Interleukin-1 beta in coronary arteries of patients with ischemic heart disease. *Arter Thromb Vasc Biol.* 1996;16(8):1000-1006.
 24. Dewberry R, Holden H, Crossman D, Francis S. Interleukin-1 receptor antagonist expression in human endothelial cells and atherosclerosis. *Arterioscler Thromb Vasc Biol.* 2000;20(11):2394-2400. doi:10.1161/01.ATV.20.11.2394
 25. Bevilacqua MP, Pober JS, Wheeler ME. Interleukin-1 activation of vascular endothelium. Effects on procoagulant activity and leukocyte adhesion. *Am J Pathol.* 1985;121(3):393-403.
 26. Libby P, Warner SJC, Friedman GB. Interleukin 1: A mitogen for human vascular smooth muscle cells that induces the release of growth-inhibitory prostanoids. *J Clin Invest.* 1988;81(2):487-498. doi:10.1172/JCI113346

27. Hou T, Tieu B, Ray S, et al. Roles of IL-6-gp130 Signaling in Vascular Inflammation. *Curr Cardiol Rev.* 2008;4(3):179-192. doi:10.2174/157340308785160570
28. Ceneri N, Zhao L, Young BD, et al. Rac2 modulates atherosclerotic calcification by regulating macrophage interleukin-1 β production. *Arterioscler Thromb Vasc Biol.* Published online 2017. doi:10.1161/ATVBAHA.116.308507
29. Ridley AJ. Rho GTPase signalling in cell migration. *Curr Opin Cell Biol.* 2015;36:103-112. doi:10.1016/j.ceb.2015.08.005
30. Heasman SJ, Ridley AJ. Mammalian Rho GTPases: New insights into their functions from in vivo studies. *Nat Rev Mol Cell Biol.* 2008;9(9):690-701. doi:10.1038/nrm2476
31. Ridley AJ. Rho GTPases and actin dynamics in membrane protrusions and vesicle trafficking. *Trends Cell Biol.* 2006;16(10):522-529. doi:10.1016/j.tcb.2006.08.006
32. Hodge RG, Ridley AJ. Regulating Rho GTPases and their regulators. *Nat Rev Mol Cell Biol.* 2016;17(8):496-510. doi:10.1038/nrm.2016.67
33. Bustelo XR, Sauzeau V, Berenjano IM. GTP-binding proteins of the Rho/Rac family: Regulation, effectors and functions in vivo. *BioEssays.* 2007;29(4):356-370. doi:10.1002/bies.20558
34. Marei H, Malliri A. Rac1 in human diseases: The therapeutic potential of targeting Rac1 signaling regulatory mechanisms. *Small GTPases.* 2017;8(3):139-163. doi:10.1080/21541248.2016.1211398
35. Garcia-Mata R, Boulter E, Burridge K. The “invisible hand”: Regulation of RHO GTPases by RHOGDIs. *Nat Rev Mol Cell Biol.* 2011;12(8):493-504. doi:10.1038/nrm3153
36. Seabra MC. Membrane association and targeting of prenylated Ras-like GTPases. *Cell*

- Signal*. 1998;10(3):167-172. doi:10.1016/S0898-6568(97)00120-4
37. Fu H, Alabdullah M, Großmann J, et al. Macrophage SR-BI mediates efferocytosis via Src/PI3K/Rac1 signaling and reduces atherosclerotic lesion necrosis. *Int J Mol Sci*. 2019;21(4):1-16. doi:10.1194/jlr.M056689
 38. McTaggart SJ. Isoprenylated proteins. *Cell Mol Life Sci*. 2006;63(3):255-267. doi:10.1007/s00018-005-5298-6
 39. Running MP. The role of lipid post-translational modification in plant developmental processes. *Front Plant Sci*. 2014;5(FEB):1-9. doi:10.3389/fpls.2014.00050
 40. Filippi MD, Harris CE, Meller J, Gu Y, Zheng Y, Williams DA. Localization of Rac2 via the C terminus and aspartic acid 150 specifies superoxide generation, actin polarity and chemotaxis in neutrophils. *Nat Immunol*. 2004;5(7):744-751. doi:10.1038/ni1081
 41. Michaelson D, Silletti J, Murphy G, D'Eustachio P, Rush M, Philips MR. Differential localization of Rho GTPases in live cells: Regulation by hypervariable regions and RhoGDI binding. *J Cell Biol*. 2001;152(1):111-126. doi:10.1083/jcb.152.1.111
 42. Didsbury JR, Uhing RJ, Snyderman R. Isoprenylation of the low molecular mass GTP-binding proteins rac 1 and rac 2: Possible role in membrane localization. *Biochem Biophys Res Commun*. 1990;171(2):804-812. doi:10.1016/0006-291X(90)91217-G
 43. Hancock JF, Magee AI, Childs JE, Marshall CJ. All ras proteins are polyisoprenylated but only some are palmitoylated. *Cell*. 1989;57(7):1167-1177. doi:10.1016/0092-8674(89)90054-8
 44. Navarro-Lérida I, Sánchez-Perales S, Calvo M, et al. A palmitoylation switch mechanism regulates Rac1 function and membrane organization. *EMBO J*. 2012;31(3):534-551. doi:10.1038/emboj.2011.446

45. Abdrabou A, Wang Z. Post-Translational Modification and Subcellular Distribution of Rac1: An Update. *Cells*. 2018;7(12):263. doi:10.3390/cells7120263
46. Bosco EE, Mulloy JC, Zheng Y. Rac1 GTPase: A “Rac” of all trades. *Cell Mol Life Sci*. 2009;66(3):370-374. doi:10.1007/s00018-008-8552-x
47. Dovas A, Couchman JR. RhoGDI: Multiple functions in the regulation of Rho family GTPase activities. *Biochem J*. 2005;390(1):1-9. doi:10.1042/BJ20050104
48. Bustelo XR, Ojeda V, Barreira M, Sauzeau V, Castro-Castro A. Rac-ing to the plasma membrane. *Small GTPases*. 2012;3(1):60-66. doi:10.4161/sgtp.19111
49. Tzima E, Del Pozo MA, Kiosses WB, et al. Activation of Rac1 by shear stress in endothelial cells mediates both cytoskeletal reorganization and effects on gene expression. *EMBO J*. 2002;21(24):6791-6800. doi:10.1093/emboj/cdf688
50. Meier B, Radeke HH, Selle S, et al. Human fibroblasts release reactive oxygen species in response to interleukin-1 or tumour necrosis factor- α . *Biochem J*. 1989;263(2):539-545. doi:10.1042/bj2630539
51. Carrizzo A, Vecchione C, Damato A, et al. Rac1 pharmacological inhibition rescues human endothelial dysfunction. *J Am Heart Assoc*. 2017;6(3). doi:10.1161/JAHA.116.004746
52. Gregg D, Rauscher FM, Goldschmidt-Clermont PJ. Rac regulates cardiovascular superoxide through diverse molecular interactions: More than a binary GTP switch. *Am J Physiol - Cell Physiol*. 2003;285(4 54-4). doi:10.1152/ajpcell.00230.2003
53. Hordijk PL. Regulation of NADPH oxidases: The role of Rac proteins. *Circ Res*. 2006;98(4):453-462. doi:10.1161/01.RES.0000204727.46710.5e
54. Williams LM, Lali F, Willetts K, et al. Rac mediates TNF-induced cytokine production

- via modulation of NF- κ B. *Mol Immunol*. 2008;45(9):2446-2454.
doi:10.1016/j.molimm.2007.12.011
55. Merad M, Martin JC. Pathological inflammation in patients with COVID-19: a key role for monocytes and macrophages. *Nat Rev Immunol*. 2020;20(6). doi:10.1038/s41577-020-0331-4
 56. Tay MZ, Poh CM, Rénia L, MacAry PA, Ng LFP. The trinity of COVID-19: immunity, inflammation and intervention. *Nat Rev Immunol*. 2020;20(6). doi:10.1038/s41577-020-0311-8
 57. García LF. Immune Response, Inflammation, and the Clinical Spectrum of COVID-19. *Front Immunol*. 2020;11. doi:10.3389/fimmu.2020.01441
 58. COVID-19 Map. Johns Hopkins University & Medicine. Published 2021. Accessed April 8, 2021. <https://coronavirus.jhu.edu/map.html>
 59. Department of Error: Clinical features of patients infected with 2019 novel coronavirus in Wuhan, China (The Lancet (2020) 395(10223) (497–506), (S0140673620301835), (10.1016/S0140-6736(20)30183-5)). *Lancet*. 2020;395(10223). doi:10.1016/S0140-6736(20)30252-X
 60. Glogauer M, Marchal CC, Zhu F, et al. Rac1 Deletion in Mouse Neutrophils Has Selective Effects on Neutrophil Functions. *J Immunol*. 2003;170(11).
doi:10.4049/jimmunol.170.11.5652
 61. Qian BZ, Li J, Zhang H, et al. CCL2 recruits inflammatory monocytes to facilitate breast-tumour metastasis. *Nature*. 2011;475(7355). doi:10.1038/nature10138
 62. Piedrahita JA, Zhang SH, Hagaman JR, Oliver PM, Maeda N. Generation of mice carrying a mutant apolipoprotein E gene inactivated by gene targeting in embryonic stem

- cells. *Proc Natl Acad Sci U S A*. 1992;89(10). doi:10.1073/pnas.89.10.4471
63. Schneider CA, Rasband WS, Eliceiri KW. NIH Image to ImageJ: 25 years of image analysis. *Nat Methods*. 2012;9(7). doi:10.1038/nmeth.2089
 64. Morrison AR, Yarovinsky TO, Young BD, et al. Chemokine-coupled β 2 integrin-induced macrophage Rac2-myosin IIA interaction regulates VEGF-A mRNA stability and arteriogenesis. *J Exp Med*. 2014;211(10). doi:10.1084/jem.20132130
 65. Davies JQ, Gordon S. Isolation and culture of murine macrophages. *Methods Mol Biol*. 2005;290. doi:10.1385/1-59259-838-2:091
 66. Lanning CC, Daddona JL, Ruiz-Velasco R, Shafer SH, Williams CL. The Rac1 C-terminal polybasic region regulates the nuclear localization and protein degradation of Rac1. *J Biol Chem*. 2004;279(42). doi:10.1074/jbc.M404977200
 67. Söderberg O, Gullberg M, Jarvius M, et al. Direct observation of individual endogenous protein complexes in situ by proximity ligation. *Nat Methods*. 2006;3(12). doi:10.1038/nmeth947
 68. Fredriksson S, Dixon W, Ji H, Koong AC, Mindrinos M, Davis RW. Multiplexed protein detection by proximity ligation for cancer biomarker validation. *Nat Methods*. 2007;4(4). doi:10.1038/nmeth1020
 69. Fredriksson S, Gullberg M, Jarvius J, et al. Protein detection using proximity-dependent DNA ligation assays. *Nat Biotechnol*. 2002;20(5). doi:10.1038/nbt0502-473
 70. Aikawa E, Nahrendorf M, Figueiredo JL, et al. Osteogenesis associates with inflammation in early-stage atherosclerosis evaluated by molecular imaging in vivo. *Circulation*. 2007;116(24). doi:10.1161/CIRCULATIONAHA.107.732867
 71. Radcliff K, Tang TB, Lim J, et al. Insulin-like growth factor-I regulates proliferation and

- osteoblastic differentiation of calcifying vascular cells via extracellular signal-regulated protein kinase and phosphatidylinositol 3-kinase pathways. *Circ Res.* 2005;96(4). doi:10.1161/01.RES.0000157671.47477.71
72. Tintut Y, Patel J, Territo M, Saini T, Parhami F, Demer LL. Monocyte/macrophage regulation of vascular calcification in vitro. *Circulation.* 2002;105(5). doi:10.1161/hc0502.102969
73. Sulciner DJ, Irani K, Yu ZX, Ferrans VJ, Goldschmidt-Clermont P, Finkel T. rac1 regulates a cytokine-stimulated, redox-dependent pathway necessary for NF-kappaB activation. *Mol Cell Biol.* 1996;16(12). doi:10.1128/mcb.16.12.7115
74. Arbibe L, Mira JP, Teusch N, et al. Toll-like receptor 2-mediated NF- κ B activation requires a Rac I-dependent pathway. *Nat Immunol.* 2000;1(6). doi:10.1038/82797
75. A PORTFOLIO OF COVID-19 PLATFORMS. The Jackson Laboratory.
76. Muñoz-Fontela C, Dowling WE, Funnell SGP, et al. Animal models for COVID-19. *Nature.* 2020;586(7830). doi:10.1038/s41586-020-2787-6
77. Zhou B, Thao TTN, Hoffmann D, et al. SARS-CoV-2 spike D614G change enhances replication and transmission. *Nature.* 2021;592(7852). doi:10.1038/s41586-021-03361-1
78. Michael Koob. B6(Cg)-Ace2tm1.1(ACE2)Mdk/J. *Jackson Lab.* Published online 2021.